Pramana – J. Phys. (2021) 95:47
https://doi.org/10.1007/s12043-021-02078-0
© Indian Academy of Sciences

EHD instability of two rigid rotating dielectric columns in porous media

GALAL M MOATIMID and MOHAMED F E AMER*

Department of Mathematics, Faculty of Education, Ain Shams University, Roxy, Cairo, Egypt
*Corresponding author. E-mail: m7md_fawzy@yahoo.com

MS received 13 June 2020; revised 25 October 2020; accepted 9 November 2020

Abstract. The present work analyses the linear azimuthal stability of a single interface between two cylindrical dielectric fluids. The theoretical model consists of two incompressible rotating electrified fluids throughout the porous media. The system is influenced by a uniform azimuthal electric field. The inner cylinder is filled with a viscous liquid. The outer one is occupied by an inviscid gas. The problem meets its motivation from a geophysics point of view. Therefore, for more convenience, the problem is considered in a planar configuration. Typically, the normal mode analysis is used to facilitate the stability approach. The examination resulted in a stream function, which is governed by a fourth-order ordinary differential equation with complicated variable coefficients. By means of the Mathematica software along with the special functions, the distribution of the stream function is written in terms of the modified Bessel functions. A non-dimensional procedure exposes some non-dimensional numbers, for instance, Weber, Ohnesorg, Taylor, Rossby and Darcy numbers. These numbers are considered with regard to the temporal and spatial increase of both frequency and modulation. The linear stability theory generated a very complicated transcendental dispersion equation. The influences of various physical parameters in the stability profile were studied as well.

Keywords. Azimuthal perturbation; rotating fluids; porous media; electrohydrodynamic stability; viscous fluids.

PACS Nos 47.20.Ib; 68.03.Kn; 47.32.Ef

1. Introduction

Electrohydrodynamics (EHD) is a field of Continuum Mechanics. It deals with the motion of media that interacts with an electric field. A comprehensive study on this topic was done by Melcher [1]. In a few words, EHD is concerned with a branch of fluid mechanics that executes together with the electrical forces. Electrodynamics is constrained by the influence of moving media on electric fields. EHD has extensive applications in several areas, for example, see EHD pump, electro-spray nanotechnology, EHD enhanced heat transfer, electro-spray mass spectrometry, etc. The basic theories underlying these applications and a brief review of the EHD advances are presented by Chen *et al* [2]. Rana *et al* [3] examined the influence of AC electric field on the onset of stability of a elstico-viscous Walters' (model B) dielectric fluid. By means of the normal modes investigation and a perturbation technique, they analysed the linear stability. They concluded that in the case of stationary convection, non-Newtonian Walters' (model B) behaves like ordinary Newtonian. One aspect of EHD incorporates the stability of two-fluid layers. Melcher and his coworkers adopted the bulk, coupled model for studying the stability that is influenced by electric fields in different situations. The interface between two miscible fluids, which have identical mechanical properties, but disparate electrical conductivities and influenced by an equilibrium tangential electric field were studied experimentally and theoretically by Hoburg and Melcher [4]. Ozen *et al* [5] examined the EHD stability of the interface between two superposed viscous fluids in a channel subject to a uniform vertical electric field. Additionally, owing to the finite conductivities of the two fluids, the interface admits surface charges. Using the Chebyshev spectral method, they have done the stability analysis for all wave numbers. The linear EHD instability of two superposed viscous dielectric fluids flowing down an inclined plane in the presence of a thermal conductivity variation and electric field were investigated by El-Sayed *et al* [6]. Using a long-wavelength approximation, a new instability was

Published online: 16 March 2021

presented.They concluded that the presence of electric field is important to prevent the drop out of the analysis when there is no stratification in thermal conductivity. Moatimid *et al* [7] analysed the linear periodic EHD stability of double cylindrical interfaces. These interfaces were separated by three incompressible viscous dielectric fluids. To relax mathematical manipulation, they adopted the viscous potential theory. They concluded that the system is governed by coupling Mathieu equations. Recently, Moatimid and Zekry [8] investigated the nonlinear instability of a non-Newtonian fluid of the Walters' B type. An axial electric field of uniform strength was pervaded along with the axis of the jet. The stability criteria, in linear as well as the nonlinear approaches, were analytically studied and numerically confirmed.

The stability of the rotating jets is of great interest because of its practical applications in liquid atomisation, breakdown of vortex cores, combustion processes, etc. Therefore, currently, many researchers are showing great interest in examining the stability of flows in a cylindrical configuration, such as cylindrical flows from cooling of rotating machinery in petroleum industry etc. Linear stability of steady flows between two rotating circular cylinders was numerically examined by Oikawa *et al* [9]. By using the pseudospectral method, they found that the critical Reynolds number increases with eccentricity. Kubitschek and Weidman [10] investigated the linear temporal instability of a uniform rotating viscous liquid column in the absence of gravity. They concluded that the rational Reynolds represents a governing parameter. Furthermore, the Hocking parameter is defined as the ratio between the surface tension and centrifugal forces. Typically, the interface stability in the presence of rotation yields a very complicated dispersion relation as the transcendental equation. Moatimid and El-Dib [11] examined EHD stability of a liquid cylinder subjected to a periodic relation. Their stability analysis was based on multiple time scales. They found that the axial electric field has a stabilising influence on the stability profile. This influence was utilised to suppress the instability of the uniform rotation. El-Dib and Moatimid [12] examined the EHD stability of a liquid cylinder subjected to a periodic rotation. They observed that in the case of a uniform rotation, if the outer cylinder is faster than the inner one, the system exhibits more stabilising influence. Their analysis, in view of multiple scales, includes resonance and non-resonance cases. Recently, El-Dib *et al* [13] examined the nonlinear Rayleigh–Taylor instability of two rotating superposed magnetic in semi-infinite media. Typically, they derived a nonlinear characteristic equation of the surface deflection. They adapted the homotopy perturbation method to investigate this equation. Additionally, they achieved an analytical approximate solution of the surface profile. El-Dib *et al* [14] introduced a new approach to study the nonlinear azimuthal instability of two rotating fluids. They used the homotopy perturbation technique to analyse the acquired nonlinear characteristic equation. Furthermore, the profile of surface deflection was theoretically possible.

Undoubtedly, the instability of fluid interfaces in porous media is a motivating force, in light of its great practical importance in many areas in physics and engineering, such as ground water hydrology, oil industry, geophysical, thermal, civil engineering, and evaporation near the surface of the ground among others. Many comprehensive studies have been showing the stability of the interface between two fluids of different densities and viscosities throughout the porous media. A viscous fluid filling the voids in a porous medium was driven by Saffman and Taylor [15]. They found that the interface between the two fluids is responsible for instability if the heavy fluid is less viscous than the other. Additionally, they showed that this condition occurs in oil fields. Nayfeh [16] presented the stability of the liquid interfaces moving with uniform velocities in homogeneous isotropic porous media. The effects of viscosity, surface tension and body forces were considered. He found that the critical conditions, separating stable from unstable disturbances, were independent of the depth of the liquid layer. Furthermore, the deviations from Darcy's law were found to be stabilising, when the flow was from the denser to the lighter fluid and vice-versa. Bau [17] investigated the interface stability of two fluid layers in fully saturated porous media. He showed that, in Kelvin–Helmholtz instability, the interface may become unstable. The corresponding conditions for marginal stability were derived for Darcian and non-Darcian flows. Bishnoi and Agrawal [18] pointed out the physical situations, where there is no necessity for modifying the inertia term when the flow and its stability obey the Darcy's law. They concluded the relation between the stability in two- and three-dimensional disturbances. A mathematical model was presented by Bhattacharyya *et al* [19] for analysing the boundary layer of an incompressible fluid past a porous plate embedded in a Darcy porous medium. The reduced nonlinear ordinary differential equations were numerically solved. In case of porous plate, they found that the fluid velocity was increased. Bhattacharyya *et al* [20] studied the effect of diffusion of chemical reactive species of an incompressible fluid over a porous flat plate in porous media. They showed that it is very important to see that in some practical chemical reaction situations, the mass absorption at the plate happens to the minor Schmidt number. The characteristics of the unsteady boundary layer flow with melting heat transfer

near a stagnation point towards a flat plate embedded in a Darcy–Brinkman porous medium with thermal radiation, were investigated by Aurangzaib *et al* [21]. They utilised similarity transformations to transform the governing partial differential equations into self-similar ordinary differential equations. The MHD stagnation-point flow and shrinking/stretching sheet in a porous medium in the presence of a heat sink/source was investigated by Seth *et al* [22]. The solutions of steady flow were obtained in higher shrinking rate due to magnetic fields and porous medium. Dual solutions for some cases of the shrinking sheet were found. Recently, Moatimid *et al* [23] examined the ferrodynamic stability of coupled horizontal interfaces between three incompressible viscous fluids. In accordance with the geophysics point of view, they considered a motion in porous media. They showed that Darcy's coefficients have a destabilising influence. Moatimid *et al* [24] investigated the influence of a uniform electric field on a streaming cylindrical sheet. They examined a few representatives of porous media. They showed that the thickness of the inner cylinder plays a dual role in the stability profile. Once more, Darcy's coefficients have a destabilising influence. Moatimid *et al* [25] examined the nonlinear stability of an interface between two magnetic fluids separated by a cylindrical interface in porous media. Their analysis accompanied a Ginzburg–Landau equation that administrated the stability criteria of the system.

The aim of the present paper is to discuss the linear stability of a rigid rotating column. The fluid column is subjected to capillary forces in the presence of an azimuthal electric field. For more convenience, the problem is assumed in a planar configuration. From a geophysics point of view, the considered theoretical model consists of a vertical cylinder, which is filled with a viscous liquid. The outer medium is assumed to extend to infinity, and is occupied by an inviscid gas. The media are saturated in porous media. The rest of the paper is arranged as follows: The statement of the problem is presented in §2. Section 3 is devoted to the method of solution. The perturbation equations and the corresponding appropriate nonlinear boundary conditions are depicted in §4. A linear characteristic dispersion relation is, also, formulated in this section. Section 5 illustrates the linear stability approach together with the consistent numerical calculations. Finally, the concluding remarks are given in §6.

2. Physical and mathematical model

A fluid saturated in a porous medium bounded by an infinite circular cylinder is considered. For more opportunities, the cylindrical polar coordinates (r, θ, z) will be utilised. The motion of two dielectric electrified fluid columns of infinite extent length is taken into account. At the equilibrium configuration, the interface profile is assumed to be of circular cross-section with radius R. The interface admits surface tension. A simple consideration of the theoretical possibilities of the structure of porous media, however, makes one realises that a general correlation between porosity and permeability do not exist. For simplicity, the porosities of the media are considered as unity. An azimuthal uniform electric field E_0 is applied. The inner column (liquid) performs a rigid viscous fluid rotation, in a weightless condition, with a uniform angular velocity Ω_1 about its axis of symmetry. This column has density ρ_1, kinematic viscosity ν_1, Darcy coefficient ξ_1 and dielectric constant ε_1. This column is embedded in a rotating unbounded fluid (gas) having density ρ_2, Darcy coefficient ξ_2, dielectric constant ε_2 and uniform angular velocity Ω_2. The tension forces act as a restoring force to otherwise damped oscillations of the interface surfaces. A schematic diagram of the configuration of the physical model is sketched in figure 1.

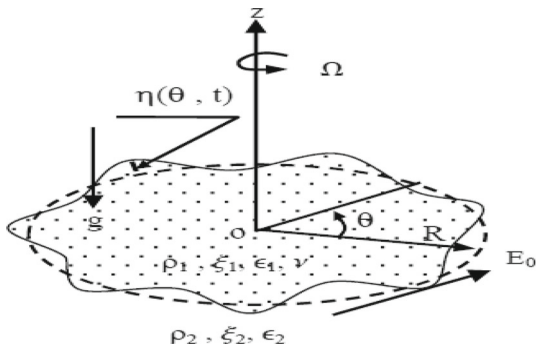

Figure 1. Schematic of the flow configuration.

The following assumptions have been adopted:

- A saturated fluid is incompressible and all physical properties of the fluid are constants.
- A porous medium is isotropic and homogeneous everywhere.
- A medium obeys the Boussinésq approximation, which states that the variation of density in the equations of motion can safely be ignored, everywhere, except in its association with the external forces.

The theory of the porous layer depends mainly on Darcy's law, which is applicable to the steady flows when the inertial effects are negligible. However, one wishes to examine a flow in which the inertial effects are included and, consequently, the derivative of the velocity will not vanish. Therefore, under such conditions, the drag on the fluid can still be approximated by Darcy's

law. Subsequently, the previous physical system satisfies the following set of governing equations:

The incompressibility condition yields

$$\nabla \cdot \underline{V} = 0. \tag{1}$$

Referring to the unit vectors along with the coordinate axes as ($\underline{e}_r$, $\underline{e}_\theta$, $\underline{e}_z$), the historical angular velocity of the fluids may be represented as $\underline{\Omega} = \Omega\,\underline{e}_z$. At this end, the governing equation of the conservation of momentum is written in the $\underline{\Omega}$ rotating frame. It is convenient to write the equation of motion in this frame of reference, which rotates with an angular velocity $\underline{\Omega}$; for illustration, see El-Dib and Moatimid [12], El-Dib *et al* [13,14] and Weidman *et al* [26]. Therefore, one gets

$$\frac{\partial \underline{V}}{\partial t} + (\underline{V} \cdot \nabla)\,\underline{V} + 2(\underline{\Omega} \wedge \underline{V}) + \underline{\Omega} \wedge (\underline{\Omega} \wedge \underline{r}) = -\frac{1}{\rho}\nabla p - g\underline{e}_z + \delta\nu\nabla^2\,\underline{V} - \xi\,\underline{V}, \tag{2}$$

where $\underline{V}$ denotes the fluid velocity relative to the rotating frame, $\partial\underline{V}/\partial t$ refers to the rate of change of $\underline{V} = (u, v, w)$ at the fixed position $\underline{r}$ in the frame and $\delta = 1$ or 0 indicates liquid or gas, respectively. The third and fourth terms are the Coriolis force and centrifugal implication, respectively, p is the pressure, g is the magnitude of the acceleration due to gravity. Furthermore, ν is the kinematic viscosity of the saturated inner fluid. The viscosity is entered throughout Darcy's resistance term as $\rho\nu\underline{V}/\kappa$, κ is the permeability constant. For simplicity, this resistance force may be written as $\xi\,\underline{V}$, where the parameter ξ is known as Darcy's coefficient.

The last term on the left-hand side of eq. (2) may be written as

$$\underline{\Omega} \wedge (\underline{\Omega} \wedge \underline{r}) = -\nabla\left[\frac{1}{2}(\underline{\Omega} \wedge \underline{r})^2\right]. \tag{3}$$

In this case, it is clear that the centrifugal term may be combined with the pressure to define the 'reduced pressure' as

$$\pi = p - \frac{1}{2}\rho(\underline{\Omega} \wedge \underline{r})^2 - \frac{1}{2}\varepsilon E_0^2\,. \tag{4}$$

Therefore, one gets

$$\frac{\partial \underline{V}}{\partial t} + (\underline{V} \cdot \nabla)\,\underline{V} + 2(\underline{\Omega} \wedge \underline{V}) = -\frac{1}{\rho}\nabla\pi + \delta\nu\nabla^2\,\underline{V} - g\underline{e}_z - \xi\,\underline{V} \tag{5}$$

In the present work, the Kelvin–Helmholtz model is adopted, so that the total velocity vector is represented by $\underline{V} = (u,\ r\Omega + v,\ w)$ where the term $r\Omega$ represents the unperturbed tangential velocity. Only two-dimensional disturbances are considered to avoid any generality loss. Therefore, one may assume that: $w = 0$.

In the equilibrium state, the equilibrium hydrostatic reduced pressure is given by

$$\pi_{0j} = -\rho_j g z + \Gamma_j, \quad j = 1,\ 2, \tag{6}$$

where the subscript (0) refers to the equilibrium state and Γ_j is the integration constant.

On the other hand, in light of the electrical part, the approximation of the electro quasistatic approximation is supposed to be true in the current problem; for instance, see Melcher [1]. Moreover, the azimuthal uniform electric field E_0 may be expressed as

$$\underline{E} = E_0\underline{e}_\theta. \tag{7}$$

For simplicity, no free currents are assumed to be present in the bulk of the liquid.

The quasistatic approximation can be understood through the indication that the fundamentals in the problem change satisfactorily slowly that the system can be taken to be in equilibrium at all times. This approximation can then be applied to areas such as classical electromagnetism, fluid mechanics, magnetohydrodynamics and thermodynamics. The objective in considering the electric fluids is concerned with the phenomena at which electric energy greatly exceeds the magnetic energy storage and, therefore, the propagating times of electromagnetic waves are short compared to those of our interest. Accordingly, Maxwell's equations may be reduced to

$$\nabla \cdot \varepsilon\underline{E} = 0 \tag{8}$$

and

$$\nabla \times \underline{E} = 0. \tag{9}$$

In accordance with the validity of the quasistatic approximation, a scalar function ϕ representing the electric potential, may be introduced as

$$\underline{E} = E_0\underline{e}_\theta - \nabla\phi, \tag{10}$$

where the scalar function ϕ satisfies the following Laplace's equation:

$$\nabla^2\phi = 0. \tag{11}$$

In accordance with the analysis, from the continuity of the normal stress at the interface $r = R$, one finds the jump in the pressure to be zero, whence:

$$\Gamma_1 - \Gamma_2 = \frac{T}{R} - (\rho_1 - \rho_2)\,gz - \tfrac{1}{2}(\varepsilon_1 - \varepsilon_2)E_0^2, \tag{12}$$

where T is the amount of surface tension. Simultaneously, as stated in the problem formulation, the motion is considered in a plane. Therefore, $\Gamma_1 - \Gamma_2$ remains constant during the motion.

3. Method of the solution

After a limited, but a finite departure from the initial configuration, the surface deflection is expressed by considering the standard normal modes analysis; for instance, see Chandrasekhar [27]. In light of this concept, the surface deflections $\eta(\theta; t)$ may be represented as a sinusoidal wave of finite amplitude, where, after disturbance, the interface, velocity and pressure are as follows:

$$r = R + \eta(\theta, t)$$

and

$$\left(u_j, v_j, \pi_j\right) = \left(U_j(r), V_j(r), \Pi_j(r)\right) \mathrm{e}^{im\theta+\omega t}, \quad j = 1, 2, \tag{13}$$

where

$$\eta(\theta, t) = \eta_0 \, \mathrm{e}^{im\theta+\omega t} \qquad (0 \le \theta \le 2\pi). \tag{14}$$

Here η_0 is the initial amplitude of the surface elevation.

Equation (14) represents the perturbations in the column radius, which determines the behaviour of the amplitude of disturbance at the interface. Moreover, the integer m is an azimuthal wavenumber, which is assumed to be a real and positive integer.

At this end, define a function $S(r, \theta; t) = r - R - \eta(\theta; t)$, where $S(r, \theta; t) = 0$ describes the wave-like profile of the disturbed interface. Therefore, the position of the disturbed interface is located at $r = R + \eta(\theta; t)$ and the unit outward normal vector to the surface becomes

$$\underline{n} = \underline{e}_r - \frac{i\,m}{r}\eta\,\underline{e}_\theta. \tag{15}$$

To examine the interface stability of the system under consideration, as stated previously, two-dimensional small disturbances are utilised in the governing equations of motion as well as the boundary conditions. Consider a small perturbation about the initial configuration of the system. The limiting case of very long longitudinal wavelength is considered here, so that the dependence of the variance on z may be neglected. Therefore, in the case of two-dimensional flow, various perturbations may be represented in the form

$$F(r, \theta, t) = \hat{f}(r) \, \mathrm{e}^{im\theta+\omega t}, \tag{16}$$

where F stands for any linear physical quantity.

For two-dimensional flow, the linearised form of equations of motion of the inner viscous fluid may be written as

$$\Delta U_1 + \left(\frac{4\Omega_1}{\nu} r^2 - 2im\right) V_1 = \frac{r^2}{\rho_1 \nu_1} \frac{\mathrm{d}\Pi_1}{\mathrm{d}r}, \tag{17}$$

$$\Delta V_1 - \left(\frac{4\Omega_1}{\nu} r^2 - 2im\right) U_1 = \frac{imr}{\rho_1 \nu_1} \Pi_1 \tag{18}$$

and

$$\frac{\partial U_1}{\partial r} + \frac{im V_1}{r} + \frac{U_1}{r} = 0, \tag{19}$$

where the operator Δ is the Laplacian operator, which may be defined as

$$\left.\begin{aligned} \Delta &= r^2 \frac{\mathrm{d}^2}{\mathrm{d}r^2} + r \frac{\mathrm{d}}{\mathrm{d}r} - (s^2 r^2 + m^2 + 1) \\ s^2 &= \frac{\omega + im\Omega_1 + \xi_1}{\nu_1} \end{aligned}\right\}. \tag{20}$$

Similarly, for the outer inviscid gas, the linearised equations of motion may be written as

$$(\omega + im\Omega_2 + \xi_2) U_2 - 4\Omega_2 V_2 = -\frac{1}{\rho_2} \frac{\mathrm{d}\Pi_2}{\mathrm{d}r}, \tag{21}$$

$$(\omega + im\Omega_2 + \xi_2) V_2 + 4\Omega_2 U_2 = -\frac{im}{\rho_2 r} \Pi_2 \tag{22}$$

and

$$\frac{\partial U_2}{\partial r} + \frac{im V_2}{r} + \frac{U_2}{r} = 0. \tag{23}$$

Typically, for a two-dimensional flow, one may identify a stream function $\psi(r, \theta; t)$ which takes the form $\psi(r, \theta; t) = \hat{\Psi}(r) \mathrm{e}^{im\theta+\omega t}$ such that

$$U_j = \frac{im}{r} \Psi_j \quad \text{and} \quad V_j = -\frac{\mathrm{d}\Psi_j}{\mathrm{d}r}, \quad j = 1, 2. \tag{24}$$

The stream function may be determined by eliminating pressure from equations of motion as given in eqs (17) and (18). For this purpose, the combination of these equations and eq. (24) yields

$$\begin{aligned} \Big(& r^4 \frac{\mathrm{d}^4}{\mathrm{d}r^4} + 2r^3 \frac{\mathrm{d}^3}{\mathrm{d}r^3} - (s^2 r^2 + 2m^2 + 1) r^2 \frac{\mathrm{d}^2}{\mathrm{d}r^2} \\ & - (s^2 r^2 - 2m^2 - 1) r \frac{\mathrm{d}}{\mathrm{d}r} \\ & + (s^2 r^2 + m^2 - 4) m^2 \Big) \Psi_1 = 0. \end{aligned} \tag{25}$$

By means of the Mathematica software (12.0.0.0) along with the special functions, the solution of the stream function may be written in terms of the modified Bessel functions, and for the purpose of the finite solution, one finds

$$\Psi_1 = C_1 r^m + C_2 \left(\frac{2m(-i)^m}{s^2} \left(I_m(sr) - \frac{(sr/2)^m}{\Gamma(m+1)} \right) \right), \quad r \le R, \tag{26}$$

where $I_m(sr)$ is the Bessel function of the first kind.

Additionally, for the outer gas, from the combination of eqs (21), (22) and (24), one finds

$$\left(r^2\frac{\mathrm{d}^2}{\mathrm{d}r^2}+r\frac{\mathrm{d}}{\mathrm{d}r}-m^2\right)\Psi_2=0. \tag{27}$$

In light of the finite solution, one finds

$$\Psi_2=C_3r^{-m},\quad r\geq R \tag{28}$$

where C_1, C_2 and C_3 are arbitrary integration constants.

They may be determined from the appropriate boundary conditions, as seen in references herein. Therefore, the complete solutions for the inner liquid outer gas, respectively, are

$$u_1=\left[imC_1\,r^{m-1}+C_2\left(\frac{2im^2(-i)^m}{s^2r}\times\left(I_m(sr)-\frac{(sr/2)^m}{\Gamma(m+1)}\right)\right)\right]\mathrm{e}^{im\,\theta+\omega t}, \tag{29}$$

$$v_1=\left[-mC_1\,r^{m-1}-C_2\left(\frac{2m(-i)^m}{s^2}\times\left(sI_m'(sr)-\frac{m(s/2)^mr^{m-1}}{\Gamma(m+1)}\right)\right)\right]\mathrm{e}^{im\,\theta+\omega t} \tag{30}$$

and

$$\begin{aligned}\pi_1=-i\rho_1\nu_1\Bigg[&C_1\,r^{m-2}\left(s^2r^2-\frac{4i\Omega_1r^2}{\nu_1}\right)\\&-\frac{2(-i)^m}{s^2r^2}C_2\left(s^3r^3I_m'''(sr)+s^2r^2I_m''(sr)\right.\\&-sr(s^2r^2+m^2+1)I_m'(sr)\\&+im\left(\frac{4\Omega_1}{\nu_1}r^2-2im\right)I_m(sr)\\&\left.+\frac{m(sr/2)^m}{\Gamma(m+1)}\left(s^2r^2-\frac{4i\Omega_1r^2}{\nu_1}\right)\right)\Bigg]\\&\times\mathrm{e}^{im\,\theta+\omega t},\end{aligned} \tag{31}$$

$$u_2=imC_3r^{-m-1}\mathrm{e}^{im\,\theta+\omega t}, \tag{32}$$

$$v_2=mC_3r^{-m-1}\mathrm{e}^{im\,\theta+\omega t} \tag{33}$$

and

$$\pi_2=i\rho_2\left(\omega+im\Omega_2+\xi_2+4i\Omega_2\right)C_3r^{-m}\mathrm{e}^{im\,\theta+\omega t}. \tag{34}$$

Returning back to the electrical part, in accordance with the two-dimensional flow considered here, Laplace's equation as given in eq. (11) that governs the electric potential ϕ may be written as

$$\left(r^2\frac{\mathrm{d}^2}{\mathrm{d}r^2}+r\frac{\mathrm{d}}{\mathrm{d}r}-m^2\right)\hat{\phi}=0, \tag{35}$$

where $\phi(r,\theta;t)$ is formulated as given in eq. (16).

Therefore, one catch the following solutions:

$$\phi_1(r,\theta,t)=C_4\,r^m\mathrm{e}^{i\,m\,\theta}\qquad(r\leq R), \tag{36}$$

and

$$\phi_2(r,\theta,t)=C_5\,r^{-m}\mathrm{e}^{i\,m\,\theta+\omega t}\qquad(r\geq R), \tag{37}$$

where C_4 and C_5 are arbitrary integration constants.

They can be determined from the convenient boundary conditions, for instance, see Melcher [1].

4. Boundary conditions and dispersion relation

The formulated boundary conditions are prescribed here at the perturbed interface $r=R+\eta(\theta,t)$. As the interface is deformed, all variables are slightly perturbed from their equilibrium values. Since the interface displacement is small, the boundary conditions on the perturbed variables need to be evaluated at the position of equilibrium rather than at the interface.

The solutions of governing equations of motion cited above are accomplished by utilising the convenient boundary conditions. At the boundary between the two fluid columns, the fluid and the electrical stresses must be balanced. The components of these fields consist of the hydrodynamic pressure, surface tension and electric stresses. These boundary conditions may be communicated as follows:

- At the interface between the two fluids, it is required that the vertical component of the fluid velocity field is continuous. This is the so-called kinematic boundary condition, which gives

$$\frac{\partial S}{\partial t}+(\underline{v}_j\cdot\nabla)S=0,\quad j=1,2\qquad\text{at }r=R+\eta. \tag{38}$$

- The shear stresses is continuous at the interface, which provides

$$\tau_{r\theta}^{(1)}=\tau_{r\theta}^{(2)}\Rightarrow\frac{\partial v_1}{\partial r}-\frac{v_1}{r}+\frac{1}{r}\frac{\partial u_1}{\partial\theta}=0,\quad\text{at }r=R+\eta, \tag{39}$$

where τ is the stress tensor due to the viscous liquid; for instance, see Chandrasekhar [27].

- The boundary conditions due to the electric field; for illustration, see Melcher [1] to acquire

$$\underline{n}\cdot\left(\varepsilon_1\underline{E}_1\right)=\underline{n}\cdot\left(\varepsilon_2\underline{E}_2\right)\Rightarrow\varepsilon_1\frac{\partial\phi_1}{\partial r}-\varepsilon_2\frac{\partial\phi_2}{\partial r}+\frac{im}{r}\eta E_0(\varepsilon_1-\varepsilon_2)=0\,,\quad\text{at } r=R+\eta \tag{40}$$

and

$$\underline{n}\times\underline{E}_1=\underline{n}\times\underline{E}_2\Rightarrow\frac{\partial\phi_1}{\partial\theta}=\frac{\partial\phi_2}{\partial\theta}\,,\quad\text{at } r=R+\eta. \tag{41}$$

- The normal stress boundary condition at the interface is given by

$$\tau_{1,rr}-\tau_{2,rr}=T\left(\frac{1}{R_1}+\frac{1}{R_2}\right)=-T\nabla.\underline{n}, \tag{42}$$

where the stress tensor is defined as

$$\tau_{ij}=-\pi\delta_{ij}+\delta\mu\left(\frac{\partial v_i}{\partial x_j}+\frac{\partial v_j}{\partial x_i}\right)+\varepsilon E_iE_j-\frac{1}{2}\varepsilon\delta_{ij}E^2. \tag{43}$$

Here R_1 and R_2 are the two radii of curvature of the interface, and μ is the dynamical viscosity.

The combination of eqs (42) and (43) produces

$$\pi_1-\pi_2-2\mu_1\frac{\partial u_1}{\partial r}-\frac{E_0}{r}\left(\varepsilon_1\frac{\partial\phi_1}{\partial\theta}-\varepsilon_2\frac{\partial\phi_2}{\partial\theta}\right)+\frac{T}{R^2}\left(1-m^2\right)\eta=0,\qquad\text{at } r=R+\eta. \tag{44}$$

Substituting from the solutions of eqs (29)–(34) and eqs (36), (37) in the above boundary conditions as given in eqs (38–41), one can achieve the constants as follows:

$$C_1=\frac{-i\,(\omega+im\Omega_1)\,\Delta_1}{mR^{m-1}\Delta_2}\eta_0, \tag{45}$$

$$C_2=\frac{(-i)^{1-m}(1-m)\,(\omega+im\Omega_1)\,s^2R^2}{mR\Delta_2}\eta_0, \tag{46}$$

$$C_3=\frac{\omega+im\Omega_2}{imR^{-m-1}}\eta_0,\quad C_4=-\frac{iE_0(\varepsilon_1-\varepsilon_2)}{R^m(\varepsilon_1+\varepsilon_2)}\eta_0,$$

$$C_5=-\frac{iE_0(\varepsilon_1-\varepsilon_2)R^m}{(\varepsilon_1+\varepsilon_2)}\eta_0, \tag{47}$$

where

$$\Delta_1=\left(s^2R^2+2m^2\right)I_m(sR)-2sRI'_m(sR)+\frac{2m(1-m)\,(sR/2)^m}{\Gamma(m+1)} \tag{48}$$

and

$$\Delta_2=\left(s^2R^2+2m\right)I_m(sR)-2sRI'_m(sR). \tag{49}$$

Substituting from the constants C_i, $i=1,\ldots,5$ as given in eqs (45)–(47), then alternates from the resulting equations into the normal stress boundary condition as given in eq. (44), keeping in mind that they are evaluated at $r=R+\eta$, after lengthy, but straightforward calculations, the following dispersion relation arise:

$$\begin{aligned}&\frac{-\mu_1\,(\omega+im\Omega_1)\,\Delta_1}{mR\Delta_2}\left(s^2R^2-\frac{4i\Omega_1R^2}{\nu_1}\right)\\&+\frac{2\mu_1(1-m)\,(\omega+im\Omega_1)}{mR\Delta_2}\\&\times\Bigg(s^3R^3I'''_m(sR)+s^2R^2I''_m(sr)\\&-sR(s^2R^2+m^2+1)I'_m(sR)\\&+im\left(\frac{4\Omega_1}{\nu_1}R^2-2im\right)I_m(sR)\\&+\frac{m(sR/2)^m}{\Gamma(m+1)}\left(s^2R^2-\frac{4i\Omega_1R^2}{\nu_1}\right)\Bigg)\\&-\frac{\rho_2}{m}\,(\omega+im\Omega_2)\,(\omega+im\Omega_2+\xi_2+4i\Omega_2)\,R\\&-\frac{2\mu_1(m-1)\,(\omega+im\Omega_1)}{R\Delta_2}\Bigg[\Delta_1-2m\Bigg(sRI'_m(sR)\\&-I_m(sR)-\frac{(m-1)(sR/2)^m}{\Gamma(m+1)}\Bigg)\Bigg]\\&-\frac{mE_0^2(\varepsilon_1-\varepsilon_2)^2}{R(\varepsilon_1+\varepsilon_2)}\\&+\frac{T}{R^2}(1-m^2)=0.\end{aligned} \tag{50}$$

Equation (50) is a very complicated transcendental equation. Actually, it contains all physical parameters that are considered in the theoretical model. At this end, the attention is focussed on the relation between the frequency of the surface waves (ω) and radius (R). For this purpose, this dispersion relation may be written in a non-dimensional form. This may be done using the following procedure:

Let $\tilde{\omega}_r=\omega_r\sqrt{\rho_1\eta_0^3/T}$ be the non-dimensional growth rate and $\tilde{\omega}_i=\omega_i\,(1/\Omega_1)$ the non-dimensional disturbance frequency. Furthermore, $\tilde{R}=R/\eta_0$ is the non-dimensional radius, $\tilde{s}=s\eta_0$, $\rho=\rho_2/\rho_1$ is the gas-to-liquid density ratio, $\Omega=\Omega_2/\Omega_1$ is the gas-to-liquid angular velocity ratio, $\mu=\mu_2/\mu_1$ is the gas-to-liquid dynamical viscosity ratio and $\varepsilon=\varepsilon_2/\varepsilon_1$ is the gas-to-liquid dielectric constant ratio. The liquid Weber number is given as: $We=\rho_1(\Omega_1\eta_0)^2\eta_0/T$. Simultaneously, Ohnesorge number is given as $Z=\mu_1/\sqrt{\rho_1T\eta_0}$, Taylor number is given as $Ta=4\Omega_1^2\eta_0^4/\nu_1^2$ and Darcy number is given by $Da=\kappa/\eta_0^2$. Moreover, the non-dimensional electric field is given as $\tilde{E}_0^2=E_0^2\,(\eta_0\varepsilon_1/T)$. It follows that $\tilde{\omega}_1=\tilde{\omega}+im\sqrt{We}$, $\tilde{\omega}_2=\tilde{\omega}+im\Omega\sqrt{We}$ and $\tilde{\omega}=\tilde{\omega}_r+i\sqrt{We}\tilde{\omega}_i$.

For more opportunities, it is necessary to introduce the physical explanation of the obtained non-dimensional parameters as follows:

- *Weber number*: It is often useful in analysing fluid flows, where there is an interface between two different fluids, especially, for multiphase flows with strongly curved surfaces.
- *Ohnesorge number*: It is used to interpret liquid viscosity in droplet formation. Its lower values represent the friction loss due to viscous forces. In contrast, its higher values yield more internal viscous dissipation.
- *Taylor number*: It characterises the importance of centrifugal forces or the so-called inertial forces due to the rotation of a fluid relative to viscous forces.
- *Darcy number*: It represents the relative effect of permeability of the medium versus its cross-sectional area, usually the diameter squared. It is found from the differential form of the Darcy's Law.

Following the previous procedure, the dispersion relation may be written as

$$
\begin{aligned}
&\frac{-\tilde{R}Z\tilde{\omega}_1\tilde{\Delta}_1}{\tilde{\Delta}_2}\left(\left(\tilde{s}\tilde{R}\right)^2-2i\tilde{R}^2\sqrt{Ta}\right)\\
&+\frac{2\tilde{R}Z(1-m)\tilde{\omega}_1}{\tilde{\Delta}_2}\\
&\times\left(\left(\tilde{s}\tilde{R}\right)^3 I_m'''(\tilde{s}\tilde{R})+\left(\tilde{s}\tilde{R}\right)^2 I_m''(\tilde{s}\tilde{R})\right.\\
&-\tilde{s}\tilde{R}\left(\left(\tilde{s}\tilde{R}\right)^2+m^2+1\right)I_m'(\tilde{s}\tilde{R})\\
&+2im\left(\tilde{R}^2\sqrt{Ta}-im\right)I_m(\tilde{s}\tilde{R})\\
&\left.+\frac{m(\tilde{s}\tilde{R}/2)^m}{\Gamma(m+1)}\left(\left(\tilde{s}\tilde{R}\right)^2-2i\tilde{R}^2\sqrt{Ta}\right)\right)\\
&-\rho\tilde{R}^3\tilde{\omega}_2\left(\tilde{\omega}_2+\frac{\mu Z}{\rho\,(Da)}+4i\Omega\sqrt{We}\right)\\
&-\frac{2\tilde{R}Zm(m-1)\tilde{\omega}_1}{\tilde{\Delta}_2}\\
&\times\left[\tilde{\Delta}_1-2m\left(\tilde{s}\tilde{R}I_m'(\tilde{s}\tilde{R})-I_m(\tilde{s}\tilde{R})\right.\right.\\
&\left.\left.-\frac{(m-1)(\tilde{s}\tilde{R}/2)^m}{\Gamma(m+1)}\right)\right]-\frac{m^2\tilde{E}_0^2\tilde{R}(1-\varepsilon)^2}{(1+\varepsilon)}\\
&+m(1-m^2)=0,
\end{aligned}
\tag{51}
$$

where

$$
\begin{aligned}
\tilde{\Delta}_1&=\left(\left(\tilde{s}\tilde{R}\right)^2+2m^2\right)I_m(\tilde{s}\tilde{R})-2\tilde{s}\tilde{R}I_m'(\tilde{s}\tilde{R})\\
&\quad+\frac{2m(1-m)\left(\tilde{s}\tilde{R}/2\right)^m}{\Gamma(m+1)},
\end{aligned}
\tag{52}
$$

$$
\tilde{\Delta}_2=\left(\left(\tilde{s}\tilde{R}\right)^2+2m\right)I_m(\tilde{s}\tilde{R})-2\tilde{s}\tilde{R}I_m'(\tilde{s}\tilde{R}) \tag{53}
$$

and

$$
\tilde{s}^2=\frac{\tilde{\omega}_1}{Z}+\frac{1}{Da}. \tag{54}
$$

As seen, eq. (51) represents the dispersion relation of the considered system. This equation controls the behaviour of the surface wave deflection. Unfortunately, its analytical compact solution cannot be controlled. For this objective, a numerical solution is needed. Consequently, the instability of the system corresponds to the positive values of the disturbance growth rate. The disturbance growth rates of different fluids can be obtained by solving this dispersion relation. Subsequently, to validate the influence of the various physical on the stability profile, a set of diagrams is established. The following calculations depend mainly on the Gaster [28] approach. Therefore, following Gaster [28] technique along with the aid of the Mathematica software as a mathematical tool, one can confirm these aspects.

5. Stability discussions and results

As per the stability analysis considered here, the instability of the rigid rotating column occurs because of the positive values of the growth rate disturbance (i.e., $\omega_r > 0$ or $\tilde{\omega}_r > 0$). This growth rate disturbance between the two media can be obtained by solving the corresponding dispersion relation as the non-dimensional dispersion relation given in eq. (51) is rather complicated. Actually, its analytical solution, in a closed-form, cannot be determined. Therefore, by using the Mathematica software, a similar argument given previously by El-Sayed *et al* [29–31] has been applied. For this purpose, in view of the Gaster [28] theorem, setting $\tilde{\omega}_i = -\tilde{R}$, takes into account $\tilde{\omega}_r = 50$, for instance, as an initial guess for the root. An iteration of the solution as ordered pairs $\left(\tilde{R}, \tilde{\omega}_r\right)$, for different values of other physical parameters included in the following investigation, is obtained. Therefore, one acquires the required data, and consequently, the required graph can be plotted. The sketched figures considered the following chosen system:

$$
\begin{aligned}
&\mu = 0.01, \quad \tilde{E}_0 = 20, \quad m = 2, \quad We = 10000\,,\\
&Z = 2.0, \quad Ta = 50.0, \quad Da = 10.0, \quad \Omega = 0.2,
\end{aligned}
$$

and

$$
\varepsilon = 1.7
$$

In what follows, figures 2–11 for a rigid rotating viscous column, are sketched. In these figures, for more accessibility, the wave growth rate is plotted vs. the radius of the column. Setting $\omega_r = 0$ or, which is addressed at the marginal state, the rigid rotating column vs. the disturbances is stable with radius value above and below

the upper and lower cut-off radius value, respectively. It is worthy to note that the cut-off radius value represents the value of the radius, where the growth rate curve crosses the radius axis in the phase plane. Only these disturbances with the radius values between the lower and upper cut-off radius values are unstable. This region can be referred to as an instability range of the rigid rotating column, and the area under the growth rate curve, in the graph of the dispersion relation, may be considered as the stability region. The domination of the radius is defined as the radius value at which the growth rate is maximum. It is very significant because it gives an indication of the ligament break-up length. In the following figures, the variation of the non-dimensional growth rate $\tilde{\omega}_r$ is plotted vs. the non-dimensional radius $\tilde{R}$.

Figure 2 is depicted to indicate the influence of Weber number We on the growth rate of the instability behaviour. In this graph, all the parameters are kept fixed except the Weber parameter We. Therefore, it has

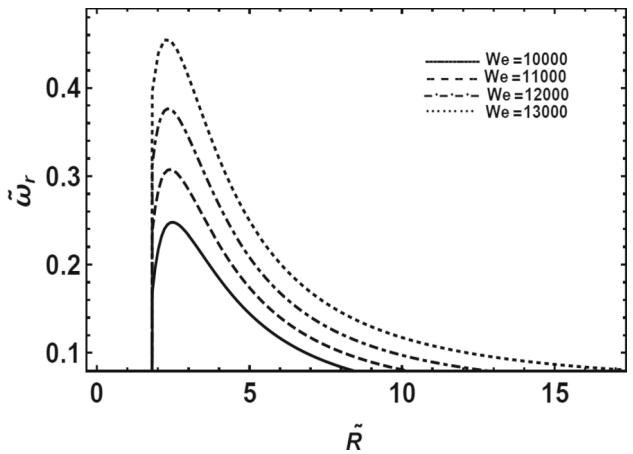

Figure 2. Plots of the variation of growth rate with radius for various values of Weber number We.

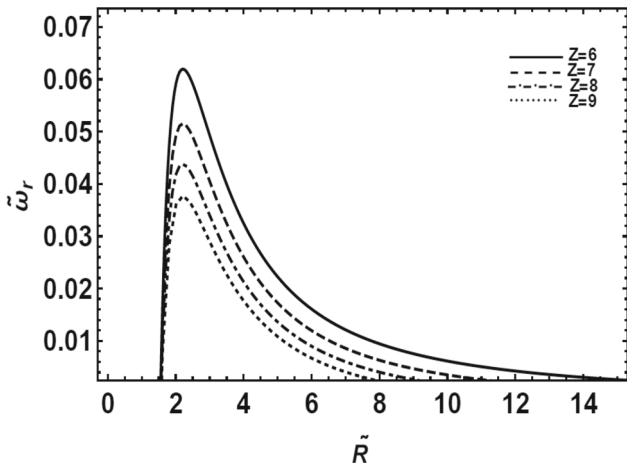

Figure 3. Plots of the variation of growth rate with radius for various values of Ohnesorge number Z.

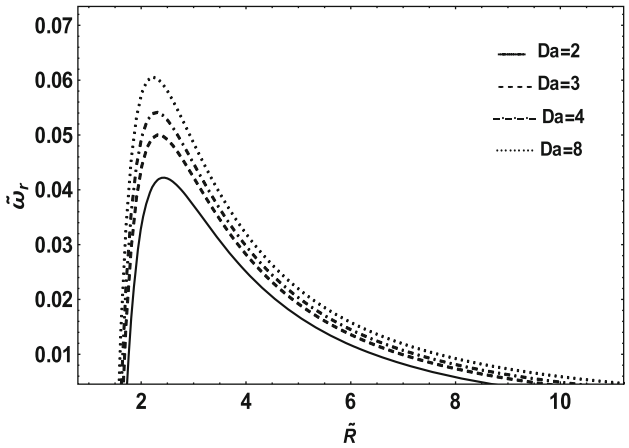

Figure 4. Plots of the variation of growth rate with radius for various values of Darcy number Da.

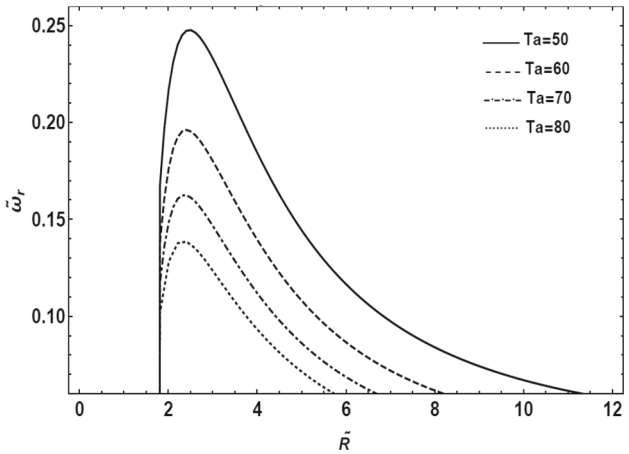

Figure 5. Plots of the variation of growth rate with radius for various values of Taylor number Ta.

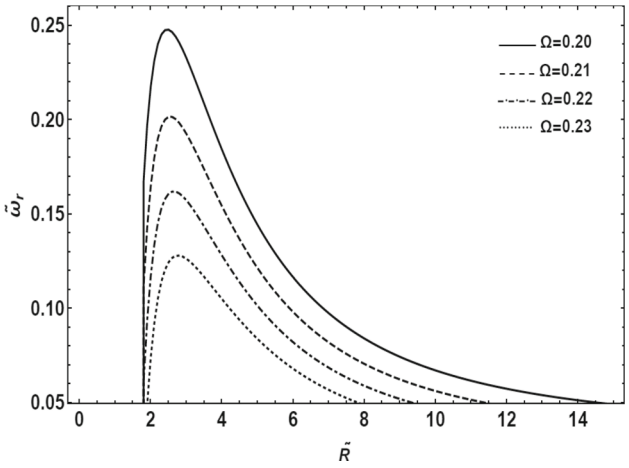

Figure 6. Plots of the variation of growth rate with radius for various values of gas-to-liquid angular velocity ratio Ω.

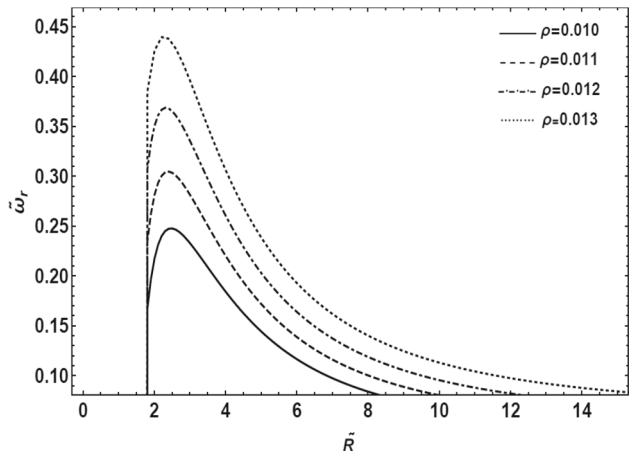

Figure 7. Plots of the variation of growth rate with radius for various values of gas-to-liquid density ratio ρ.

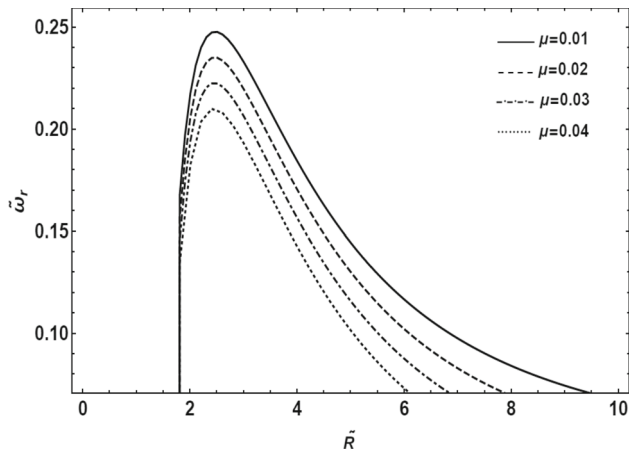

Figure 8. Plots of the variation of growth rate with radius for various values of gas-to-liquid dynamic viscosity ratio μ.

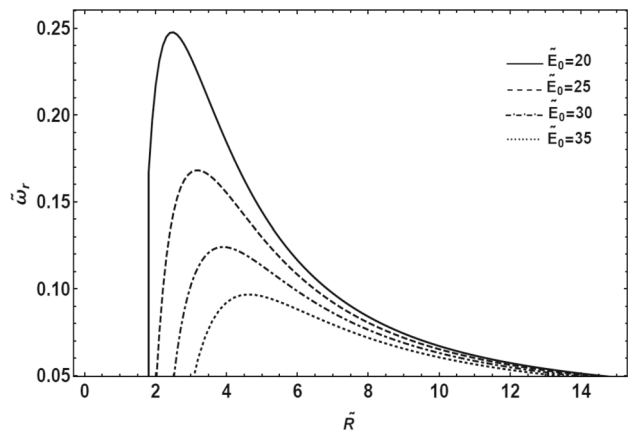

Figure 9. Plots of the variation of growth rate with radius for various values of electric field $\tilde{E}_0$.

many consecutive values. It is seen that as *We* increases, both maximum growth rate and the upper cut-off radius

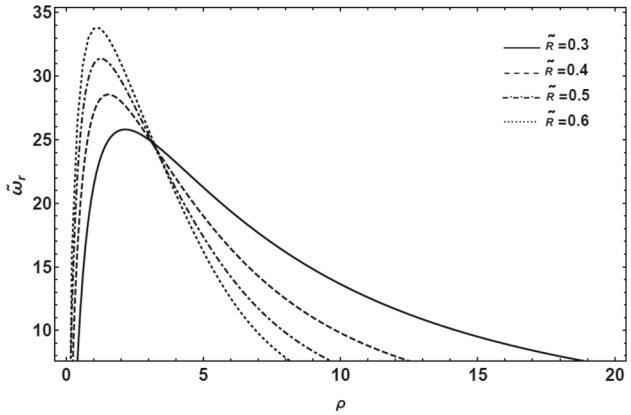

Figure 10. Plots of the variation of growth rate with gas–to-liquid density ratio for various values of radius.

also increase. Moreover, from the definition of *We*, it is noted that an increase in *We* may be caused either by an increase in the initial angular velocity, or density, or by decrease in surface tension of the liquid. On the other hand, both the lower cut-off and the dominant radius value remain constant. This shows a destabilising influence on *We*. This result is in good agreement with the result confirmed by El-Sayed *et al* [29–31].

Figure 3 indicates the viscous effects on the disturbance growth rate. The curves are depicted in the asymmetric case, as $m = 2$. It is evident that the growth rate decreases with the increase in Ohnesorge number, especially, when column radius is large, which represents the viscous effects. As shown in this figure, as Ohnesorge number Z is increased, the values of the growth rate of disturbances are dramatically reduced, as a result of the increased liquid viscosity. Therefore, the liquid viscosity as well as Z have stabilising effects on the considered system. This implies that the viscosity can dampen the instability of the rigid rotating column. It is worthy to note that, since Z denotes the ratio of the viscous forces to surface tension force, a smaller Z indicates that viscous force is smaller than the surface tension force, and in this case, the growth rate is higher. This makes sense because surface tension is responsible for driving the instability. Note that both the maximum growth rate and the instability region are decreased, when Z increases. Similar results were found in previous studies, for instance, see Li [32] and El-Sayed *et al* [29].

Figure 4 shows the effect of Darcy number (*Da*) (non-dimensional medium permeability) on the stability profile of the considered system. It is clear that the system is stable for radius less than 1.5, i.e. $\tilde{R} \leq 1.5$, and for values greater than 11, i.e. $\tilde{R} \geq 11$, in the considered system. By increasing *Da*, both the maximum growth rate and the corresponding upper cut-off radius values are increased. On the other hand, the dominance and lower cut-off radius values are decreased. Therefore, the

medium permeability as well as *Da* have destabilising effects on the considered system. Physically, this phenomenon can be explained as *Da* is equal to κ/η_0^2, where κ is the permeability of the porous medium. This means that increasing the values of *Da* causes an increase in permeability of the porous medium, which in turn facilitates the streaming velocity of the fluid flow. Also, when the streaming velocity increases, the instability of the system is increased. In other words, when the permeability of the medium increases, the holes of the porous medium are very large and the resistance of the medium may be neglected so that the streaming velocity increases and causes instability of the system. This result is in good agreement with the result confirmed by Moatimid and Hassan [33].

The effect of rotation on the rigid-rotating column, for various values of Taylor number Ta, of the non-dimensional growth rate $\tilde{\omega}_r$ vs. the non-dimensional radius $\tilde{R}$, when $m = 2$, is displayed in figure 5. It is seen that as Taylor number Ta is increased, the values of the growth rate of disturbances and the upper cut-off radius are substantially reduced. Therefore, one can prove that the absence of rotation makes the viscous rigid-rotating column more unstable than its presence. Moreover, the lower cut-off radius values remain constant, but the dominant radius values decrease with the increase of *Ta*. Furthermore, Ta as well as Z have stabilising effects on the system. This result is in good agreement with the result confirmed by Fu *et al* [34,35], where they confirmed that Rossby number $R_0 = UL/\Omega$ has destabilising effect. It is well known that the increase of R_0 is obtained by decreasing the rotation, i.e. the rotation of the liquid ($Ta = 4\Omega_1^2\eta_0^4/\nu_1^2$) has stabiliing effect.

In figure 6, the non-dimensional growth rate $\tilde{\omega}_r$ is drawn as a function of non-dimensional radius $\tilde{R}$ for various values of Ω. It is observed from figure 6 that the increase of the gas-to-liquid angular velocity ratio (rotation ratio) Ω leads to a decrease in growth rate and upper cut-off radius values. This indicates that an increase in the ambient gas angular velocity enhances stability of viscous rigid rotating column, which means that a low ambient gas angular velocity enhances the liquid atomisation. Therefore, one concludes that the gas-to-liquid angular velocity ratio also has a stabilising effect on the system. This result is compatible with similar results obtained by El-Dib *et al* [14].

The effect of gas-to-liquid density ratio ρ on wave growth rate $\tilde{\omega}_r$ is examined in figure 7. From this figure, it is observed that, when the gas-to-liquid density ratio increases, both the growth rate and the instability range of disturbances as well as the upper cut-off radius values are dramatically increased. Additionally, the dominant radius value decreases by the increase of this parameter. On the other hand, the lower cut-off radius values is constant due to the increase of this parameter. Furthermore, it can be seen that *We* is unchanged by increasing this parameter, which implies that there is an increase in the gas density ρ_2. Therefore, it may be concluded that the high ambient gas density enhances the instability of the viscous column. Therefore, the gas-to-liquid density ratio has a destabilising effect on the considered system, which conforms to the results of Brenn *et al* [36].

Figure 8 shows the variation of non-dimensional growth rate $\tilde{\omega}_r$ vs. the non-dimensional radius $\tilde{R}$ for some values of the gas-to-liquid dynamic viscosity ratio μ. It is evident from this figure that as μ increases, the maximum growth rate and the upper cut-off as well as the dominant radius values decrease. Meanwhile, the lower cut-off radius values remain nearly constant at the given conditions. Therefore, the gas-to-liquid dynamical viscosity ratio has stabilising effect. It is observed that the liquid Ohnesorge number is unchanged, which implies that there is an increase in the dynamical viscosity of the gas μ_2. Therefore, it may be concluded that the high ambient gas dynamical viscosity enhances the stability of the viscous column. Similar results can be found in previous studies (see El-Sayed *et al* [30]).

Figure 9 shows the variation of non-dimensional growth rate $\tilde{\omega}_r$ as a function of non-dimensional radius $\tilde{R}$ for various values of electric field parameter $\tilde{E}_0$, when $m = 2$. From this figure, it is observed that the effect of electric field on the growth rates of waves is similar to the effects of Ohnesorge and Taylor numbers as given in figures 3 and 5. Additionally, it is clear that as $\tilde{E}_0$ is increased, the values of the growth rate of disturbances and the instability region are substantially reduced. Moreover, the maximum growth rate and the upper cut-off radius values decrease by the increase of the electric field parameter, while the dominant and lower cut-off radius values increase with the increase of the electric field parameter. Therefore, one can conclude that the applied electric field has a stabilising effect on the considered system. This result has been verified earlier by many researchers. For instance, it coincides with the previously published results by El-Sayed *et al* [29].

Figure 10 shows the variation of non-dimensional growth rate $\tilde{\omega}_r$ with density ratio ρ for some values of non-dimensional column radius $\tilde{R}$. It is evident from this figure that as $\tilde{R}$ increases, the maximum growth rate increases, but the dominant and the lower as well as the upper cut-off density ratio values decrease. Additionally, $\tilde{R}$ has a dual role in the stability of the considered system destabilising and then becomes stabilising after a critical density ratio value, which is approximately equal to 3.2.

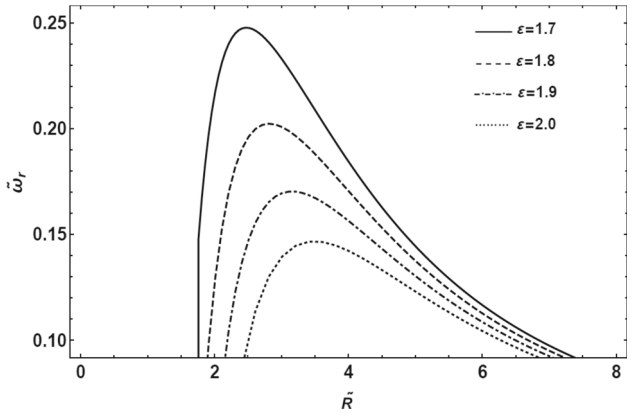

Figure 11. Plots of the variation of growth rate with radius for various values of gas-to-liquid dielectric constant ratio ε.

Figure 11 depicts the non-dimensional growth rate $\tilde{\omega}_r$ vs. the non-dimensional radius $\tilde{R}$ for various values of gas-to-liquid dielectric constant ratio ε, when $m = 2$. From this figure, it is observed that the effect of this parameter is similar to the effects of the electric field, Ohnesorge and Taylor numbers as given in figures 3, 5 and 9. Additionally, it is clear that as ε is increased, the values of the growth rate of disturbances and the instability region are substantially reduced. Moreover, the maximum growth rate and the upper cut-off radius values decrease by increasing this parameter. Meanwhile, the dominant and lower cut-off radius values increase by increasing the gas-to-liquid dielectric constant ratio. Furthermore, it can be seen that the non-dimensional electric field E_0 is unchanged by increasing this parameter, which implies that there is an increase in the dielectric constant of the ambient gas ε_2. Therefore, it may be concluded that the lower ambient gas dielectric constant enhances the instability of the viscous column. Therefore, one can conclude that the gas-to-liquid dielectric constant ratio has a stabilising effect on the considered system. This result has been verified earlier by many researchers (see El-Sayed *et al* [37]).

6. Concluding remarks

The present paper scrutinised the linear stability analysis of two rotating cylindrical, homogeneous and incompressible electrified fluids, separated by a circular interface. The inner fluid is occupied by a viscous fluid and the outer one is filled with an inviscid gas. The system is pervaded by a uniform azimuthal electric field. In accordance with the importance of porous media, the work examines a few representatives of the porous media. To relax the mathematical manipulation, a simplified formulation is considered in a planner geometry. Therefore, the stream function is adopted. This function is governed by a very complicated fourth-order differential equation with variable coefficients as given in eq. (25). A coupling of the Mathematica software together with the special functions is utilised to obtain a theoretical solution of the stream function. The boundary-value problem reveals an intricate and complicated transcendental dispersion relation as given in eq. (51). A non-dimensional analysis reveals that some non-dimensional numbers such as Weber, Ohnesorge, Taylor, Rosseby and Darcy numbers are arisen. By means of the Gaster theorem [28], with the aid of the Mathematica software, a numerical solution to this equation has been accomplished. The concluding remarks may be drawn as follows:

- The non-dimensional column radius $\tilde{R}$ has a dual role in the stability of the considered system. As the gas-to-liquid density ratio $\rho \leq 3.2$, the radius values have destabilising effect. On the other hand, when the gas-to-liquid density ratio $\rho \geq 3.2$, the radius values have stabilising effect. Therefore, a dramatically dual role of the radius has been obtained.
- The parameters of the electric field $\tilde{E}_0$, viscous effect through Ohnesorge number Z, the rotation effect through Taylor number Ta, gas-to-liquid rotation ratio Ω, gas-to-liquid dynamic viscosity ratio and the ratio of the dielectric constant between the gas-to-liquid have stabilising influence on the considered system.
- Weber number We, Darcy number Da and gas-to-liquid density ratio ρ have destabilising effects on the considered system, producing a higher growth rate and thus a shorter break-up time.

References

[1] J R Melcher, *Field coupled surface waves* (Camdridge University Press, New York, 1963)
[2] X Chen, J Chen and X Yin, *Chin. Sci. Bull.* **48**, 1055 (2003)
[3] G C Rana, R Chand and D Yadav, *FME Trans.* **43**, 154 (2015)
[4] J F Hoburg and J R Melcher, *J. Fluid Mech.* **73**, 333 (1976)
[5] F Li Ozen, N Aubry, D T Papageorgious and P G Petropoulos, *J. Fluid Mech.* **583**, 347 (2007)
[6] M F El-Sayed, G M Moatimid and N M Hafez, *Prog. Appl. Math.* **2**, 33 (2011)
[7] G M Moatimid, Y O El-Dib and M H Zekry, *Chin. J. Phys.* **56**, 2507 (2018)
[8] G M Moatimid and M H Zekry, *Micro. Tech.* **26**, 2013(2020)
[9] M Oikawa, T Karasudani and M Funakoshi, *J. Phys. Soc. Jpn.* **58**, 2355 (1989)
[10] J P Kubitschek and P D Weidman, *J. Fluid Mech.* **572**, 261 (2007)

[11] G M Moatimid and Y O El-Dib, *Int. J. Eng. Sci.* **32**, 1183 (1994)
[12] Y O El-Dib and G M Moatimid, *Physica A* **205**, 511 (1994)
[13] Y O El-Dib, G M Moatimid and A A Mady, *Pramana – J. Phys.* **93**: 82 (2019).
[14] Y O El-Dib, G M Moatimid and A A Mady, *Chin. J. Phys.* **66**, 285 (2020)
[15] P G Saffman and G I Taylor, *Proc. R. Soc. A* **245**, 312 (1958)
[16] A H Nayfeh, *Phys. Fluids* **15**, 1751 (1972)
[17] H H Bau, *Phys. Fluids* **25**, 1719 (1982)
[18] J Bishnoi and S C Agrawal, *Ind. J. Pure Appl. Math.* **22**, 611 (1991)
[19] K Bhattacharyya, S Mukhopadhyay and G C Layek, *J. Pet. Sci. Eng.* **78**, 304 (2011)
[20] K Bhattacharyya, M S Uddin, G C Layek and W Alipk, *Chem. Eng. Commun.* **200**, 1701 (2013)
[21] M K Aurangzaib, K Bhattacharyya and S Shafie, *Nonlinear Eng.* **5**, 99 (2016)
[22] G S Seth, A K Singha, M S Mandal, A Banerjee and K Bhattacharyya, *Int. J. Mech. Sci.* **134**, 98 (2017)
[23] G M Moatimid, N T Eldabe and A Sayed, *Heat Transf.-Asian Res.* **48**, 4074 (2019)
[24] G M Moatimid, Y O El-Dib and M H Zekry, *Pramana – J. Phys.* **92**: 22 (2019)
[25] G M Moatimid, Y O El-Dib and M H Zekry, *Arab. J. Sci. Eng.* **45**, 391 (2020)
[26] P D Weidman, M Goto and A Fridberg, *ZAMP* **48**, 921 (1997)
[27] S Chandrasekhar, *Hydrodynamic and hydromagnetic stability* (Camdridge University Press, New York, 1961)
[28] M Gaster, *J. Fluid Mech*. **14**, 222 (1962)
[29] M F El-Sayed, G M Moatimid, F M F Elsabaa and M F E Amer, *At. Sprays* **26**, 349 (2016)
[30] M F El-Sayed, G M Moatimid, F M F Elsabaa and M F E Amer, *J. Porous Media* **19**, 751 (2016)
[31] M F El-Sayed, G M Moatimid, F M F Elsabaa and M F E Amer, *Int. J. Fluid Mech. Res*. **44**, 93 (2017)
[32] X Li, *At. Sprays* **5**, 89 (1995)
[33] G M Moatimid and M A Hassan, *Int. J. Eng. Sci.* **54**, 15 (2012)
[34] Q-F Fu, B-Q Jia and L-J Yang, *Int. J. Heat Mass Transf.* **104**, 644 (2017)
[35] Q-F Fu, X-D Deng, B-Q Jia and L-J Yang, *AIAA J*. **56**(**7**), 2615 (2018)
[36] G Brenn, Z Liu and F Durst, *Int. J. Multiph. Flow* **26**, 1621 (2000)
[37] M F El-Sayed, G M Moatimid, F M F Elsabaa and M F E Amer, *Int. Phenom. Heat Transf.* **3**, 159 (2015)